Automotive Experiences
Vol. 7 No. 2 (2024) pp. 284-298
p-ISSN: 2615-6202 e-ISSN: 2615-6636

Research Paper

Experimental Investigation of Using Thermoelectric Coolers under Different Cooling Methods as An Alternative Air Conditioning System for Car Cabin

Ragil Sukarno[1], **Agung Premono**[1], **Yohanes Gunawan**[2], **Apri Wiyono**[3], **Ahmad Lubi**[1]

[1]Department of Mechanical Engineering, Universitas Negeri Jakarta, Jakarta Timur 13220, Indonesia
[2]Polytechnic of Energy and Mineral Akamigas, Ministry of Energy and Mineral Resources (KESDM), Cepu, Blora, Central Java 58315, Indonesia
[3]Department of Automotive Engineering Education, Faculty of Technology and Vocational Education, Universitas Pendidikan Indonesia, Bandung 40154, Indonesia

ragil-sukarno@unj.ac.id

https://doi.org/10.31603/ae.11485

Published by Automotive Laboratory of Universitas Muhammadiyah Magelang

Article Info
Submitted:
02/06/2024
Revised:
09/08/2024
Accepted:
18/09/2024
Online first:
18/09/2024

Abstract

The cabin car temperature will increase when parked in direct sunlight, so the energy required to cool cabin space by the air conditioner will be higher. This study aims to investigate using a thermoelectric cooling system as an alternative to a chiller system to supply cold air to the car cabin under different cooling methods for parked cars. Experimental testing of thermoelectric cooling systems was conducted to produce cold air that can be applied to car cabins as an alternative to conventional air conditioners. The thermoelectric cooling system was varied with single and double TEC modules. The double TEC modules are arranged in a series of electrical and parallel thermal arrangements. A cooling water block using a mixture of water and ethylene glycol with variations of 0.4 lpm, 0.5 lpm, and 0.6 lpm was added to the hot side of the thermoelectric module. The result shows that the thermoelectric cooling system can work properly during the 2-hour test, which constantly supplies air to the cabin space between 20-25 °C, depending on the configuration of the cooling system. The highest COP of 0.84 was obtained when using the double TEC with heatsink and added 0.5 lpm water cooling system, while the lowest COP of 0.53 was obtained when using the single TEC module without a cooling water block.

Keywords: Cabin car; Thermoelectric cooling; Cooling water block; COP

1. Introduction

The car cabin temperature will increase when parked under the direct sun, which means this extreme increase in car cabin temperature requires more energy consumption to operate the air conditioner [1], [2]. In addition, the drastic increase in temperature inside the vehicle cabin affects human comfort [1], [3], so an air conditioning system is needed to give thermal comfort to passengers. The energy consumption for operating an air conditioning system is high, so improving energy efficiency is essential [2]–[5]. Many studies have been conducted to develop cooling systems for parked cars. Setiyo M. et al. [6] utilized an evaporative cooling system to circulate ambient air from the environment into the vehicle cabin. The results showed that circulating fresh air with an existing fan in the car can reduce the vehicle cabin temperature to 9.8 °C. Su, Wang, et al. [7] also tried to reduce energy consumption for cooling systems in commercial vehicles, who conducted a computational fluid dynamics simulation of a localized driver thermoelectric air conditioning system. The cooling system consists of a TEC1-12706 module, centrifugal fans, heat exchangers, and a circulating water pump installed outside the thermal heat exchanger. The results show that when the air supply temperature

is 16 °C, air velocity is 5 m/s, and the constant ambient temperature conditions result in maximum comfort for the driver.

To improve the energy efficiency of the car cabin cooling system, many researchers have investigated using local air conditioning systems with thermoelectric chillers to avoid significant energy waste. Wan, Su et al. [8] proposed a local air conditioning system using thermoelectric coolers (TECs) customized around the driver. The results show that the cooling system can meet the driver's thermal comfort requirements. Thermoelectric cooling systems are widely used for several advantages: lightweight, low noise, no refrigerant, compact, easy to use, and fast cooling technology [9]–[12]. The working principle of a thermoelectric cooler (TEC) is based on the Peltier effect, which directly converts electrical energy into TEC's temperature difference. The heat from the cold side of the TEC will be absorbed and transferred to the hot side of the TEC to be released so that the air on the cold side of the TEC will be cooled [10], [13], [14].

The cooling system's performance can be achieved by increasing the heat transfer on the hot side of the TEC and increasing the number of TEC modules and positions [15]–[17]. Heat transfer enhancement can be done by adding a heatsink on the hot side of the thermoelectric. Mirmanto et al. [17] conducted experiments on several variations of thermoelectric positions in cooling box applications, in which the size was 215 mm x 175 mm x 130 mm, and the wall thickness was 50 mm. Thermoelectrics were at the top, on the bottom, and on the wall. The results showed that TEC placement on the wall gave the best results, and the COP decreased with operation time. Ma, Zuo et al. [18] Investigated the performance of a single TEC module as a portable thermoelectric cooling system for local human body cooling and compared the optimal operational voltage. The maximum cooling capacity was 26.7 W, and COP = 0.92 was obtained at the best operating voltage, 10V. Ang, Ng et al. [19] investigated single-stage and multi-stage TEC performance as a cooling wearable device. The results showed that multi-stage TECs have the potential to provide more cooling capacity, which promotes more cooling sensation on human skin. Studies to compare the effect of using different numbers of modules were also conducted by Ahmed et al. [20]. Increasing the number of TEC modules will increase the cabin's heat transfer capability, thereby reducing cabin temperature. However, increasing the number of TEC modules must be followed by the input power availability, which also increases. Increasing the number of TEC modules without increasing the total input power will reduce each TEC module's input power and will cause a decrease in the TEC cooling system. Therefore, the source of electricity for cooling must be sufficient to get the impact of increasing the number of TEC modules.

In addition to increasing heat transfer and the number of thermoelectric modules, modifying the structure of the heat transfer area can also improve the performance of a thermoelectric cooler. Qiu et al. [21] conducted qualitative and quantitative analyses to examine the factors influencing the thermoelectric cooler performance with a non-uniform cross-section. The results show that, compared to a thermoelectric cooler featuring a uniform cross-section, the optimized thermoelectric cooler with a non-uniform cross-section increases 35.73% in cooling capacity and 21.59% in Coefficient of performance. Chen et al. [22] conducted a combined mathematical modeling and experimental study. They designed a segmented converging structure for a heat exchanger at various angles to extract heat with a thermoelectric generator. This study also examined the impact of temperature and air mass flow on predicting backpressure power loss and the heat exchanger's performance sensitivity. Compared to a conventional plate-type heat exchanger, the segmented converging thermoelectric generator demonstrated a 12.5% increase in output power and a 14.8% reduction in backpressure power loss. Ang et al. [19] performed an analysis using finite element analysis (FEA) to examine the impact of multi-stage thermoelectric coolers (TECs) on performance, especially on achieving lower cold-side temperatures and optimizing the Coefficient of performance (COP). The findings indicate that multi-stage TECs could enhance the thermal comfort of human skin while controlling the power required per unit of cooling capacity. Liu et al. [23] compared the structural arrangements of thermoelectric coolers, specifically the cubic two-stage TEC, square-type two-stage TEC, and pyramid-type two-stage TEC to determine the

optimal thermal performance. Their study revealed that C-TTEC exhibited the lowest temperature on the cold side compared to P-TTEC and S-TTEC, respectively.

Another method to enhance the performance of a thermoelectric cooler involves incorporating additional devices, such as a vapor chamber based on heat pipe principles, along with additional instrumentation for more efficient control of the cooling system. Winarta et al. [24], experimented using a thermoelectric cooler box equipped with a vapor chamber to enhance heat absorption on the hot side effectively. Their investigation concluded that higher DC-ampere supply adjustments to the thermoelectric cooler resulted in lower temperatures within the cooler box. Furthermore, the experiment showed the highest Coefficient of performance (COP) achieved when the electric current was set to 4 Amperes. Midiani et al. [25] conducted a study to investigate the performance of thermoelectric coolers with and without a fan on the cold side. The results indicated that using a fan can optimize cabin temperature distribution and enhance the thermoelectric cooler's heat transfer performance on the cold side. Elarusi et al. [26] introduced an innovative system design incorporating an optimal cooling or heating input current. This system is installed before the vehicle's heating, ventilation, and air conditioning (HVAC) system becomes active. It includes a car seat climate control (CSCC) design with two heat pumps placed in the backrest and seatback. Furthermore, in the research conducted by [27], the result of the COP or efficiency of the Thermoelectric cooling system is measured 0.05-0.07. The lowest temperature achieved by the thermoelectric cooling system is 27 °C.

Recent research has extensively explored the application of thermoelectric generators that utilize the heat generated in motorized vehicles. This heat is then coupled with a thermoelectric cooler to provide vehicle cooling. Kim et al. [28] utilized twelve thermoelectric generators to harness heat from the internal combustion engine's exhaust to generate electricity. This electricity was then used to operate a cooling system, enhancing the comfort of the car's air conditioning. Their research found that the cooling system could reduce the cabin temperature from 45 °C to 26 °C in less than three minutes, requiring a power input of 90.715 watts. Al-Amir et al. [29], designed a cooling system that utilizes a thermoelectric cooler powered by exhaust gases from a diesel engine. They reported a 17% reduction in fuel consumption when using the thermoelectric cooler compared to a system without this technology. Using waste heat energy to generate power in vehicles through Thermoelectric Generators (TEG) to enhance the cooling performance of electric motors and meet braking requirements has seen widespread development [30].

A literature review shows that increased heat transfer on the hot side of TEC significantly impacts the cooling system's performance. In application, TECs still need to be applied to air conditioning systems of car cabins. Therefore, this study investigates the use of a thermoelectric cooling system as an alternative to a chiller system to divert the function of a conventional air conditioner that supplies cold air on the evaporator side into the cabin of a parked car. This study also tested whether the thermoelectric-based cooling system can work constantly for a certain period while the vehicle is parked through a 2-hour test. In addition, the effects of single-TEC and double-TEC arrangement variations and the use of cooling water blocks on the cooling system performance and energy efficiency were also investigated.

2. Methods

2.1. Experimental Setup

Air conditioning systems in cars generally use conventional (compression) air conditioning, which consists of a compressor, condenser, expansion valve, and evaporator. To cool the car cabin, fresh air or recirculated air from inside the cabin will be passed by the blower through the evaporator grille so that the air entering the vehicle cabin becomes cold, as shown in **Figure 1a**. The conventional AC system usually works when the vehicle is running. However, the engine is off when the car is parked, so the AC system doesn't work. If the vehicle is parked in an open space under direct sunlight for a long time, the temperature in the cabin will rise significantly and even exceed the ambient temperature. In this study, an alternative thermoelectric cooling system is designed to switch the function of conventional AC that supplies cold air on the evaporator side, as shown in **Figure 1b**. The cold

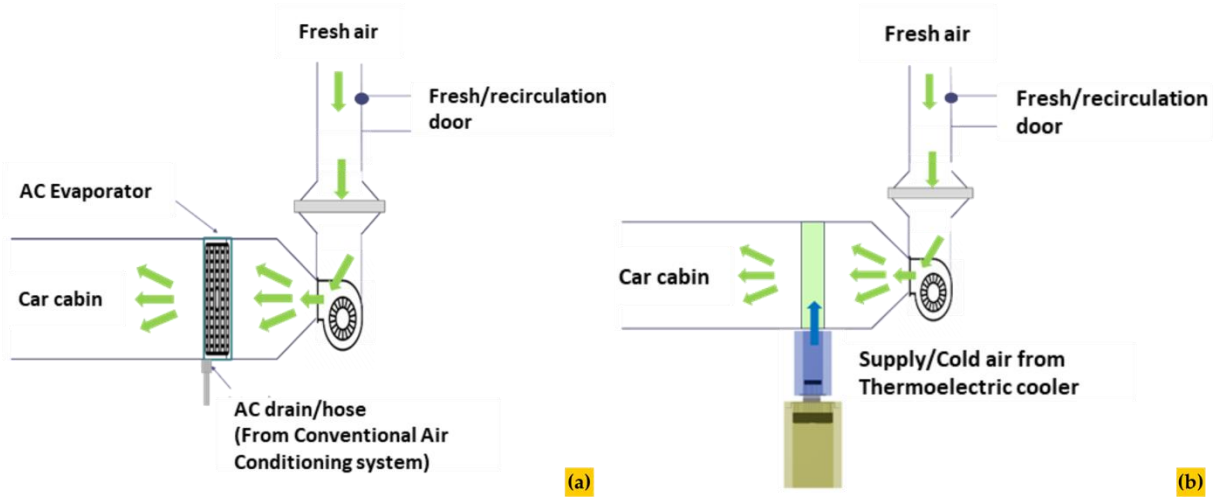

Figure 1. (a) Air conditioning circulation in conventional AC [31]; (b) Thermoelectric cooling proposed for car cabin

air obtained from the thermoelectric cooler can be used as an alternative cooling to supply cold air to the cabin car while parked.

The experimental testing of a thermoelectric cooling system will be carried out to produce cold air that can be applied to car cabins as an alternative to conventional air conditioners. The thermoelectrical cooling system consists of supply air ducting, hot side and cold side ducting, thermoelectric module TEC1-12706, the aluminum heatsinks on the hot and cold side, an axial fan on the hot and cold side, and power supply to generate DC current. Ducting is made of a Polyurethane duct with a thickness of 20 mm; on the air supply side, the inner size is 40 mm x 40 mm x 180 mm (WxHxL), while the exhaust heat duct measures 92 mm x 92 mm x 180 mm (WxHxL) (**Figure 2**). The air velocity in the hot side and cold side of the ducting was kept constant at 2 m/s. Thermal paste with a thermal conductivity of 12.6 (W/m.K) is added between TEC and the heat sink to increase heat transfer by reducing the air-gap resistance between both surfaces. This study also investigated the effect of using cooling water blocks on the hot side of the TEC to release heat on the hot side of TEC and thermoelectric cooling performance, as shown in **Figure 3**. A water-ethylene glycol mixture radiator coolant was used as a liquid coolant for the cooling water block. Using a Water-ethylene glycol mixture is based on considering its advantages, which are lower freezing and higher boiling points. This coolant can be used against freezing and overheating and can work optimally to keep the TEC hot side temperature as low as possible [32], [33].

Liquid from the tank is pumped to the entrance side of the water block so that the heat from the hot side of the TEC will be absorbed by the liquid and then flow into the radiator. The fluid that enters the radiator will be cooled by convection, flowed into the storage tank, and then pumped again to the water block.

A DC voltage regulator controls the pump voltage to regulate the liquid flow rate so that the water flow rate varies depending on the voltage applied to the pump. The coolant flow rate varies at 0.4 lpm, 0.5 lpm, and 0.6 lpm with adjustments to the DC voltage of 5 V, 6 V, and 7 V, respectively. After flowing into the block, water temperature increases, which means that heat from the hot side TEC has been transferred to the liquid before being transmitted through the heatsink. This study tested the performance of a single TEC and double TEC arranged in a series of electrical and parallel thermal, as shown in **Figure 4**. On the hot side of the TEC, an aluminum heatsink and a combination of the aluminum heatsink and liquid block were used (**Figure 5**). This study used a water-ethylene glycol mixture coolant with a flow rate of 0.4 lpm, 0.5 lpm, and 0.6 lpm.

The temperature measurement uses a K-type thermocouple connected to a Lutron LUTRON TM-947SD digital thermometer with an accuracy of ±0.1 °C. The placement of thermocouples is shown in **Figure 6**. Measurement data is recorded in the digital thermometer via SD card. Data was recorded for 7200 s for each variation, assuming the car was parked for at least 2 hours. This is conducted to determine the thermoelectric cooling system performance system while

working for 2 hours. Voltage, current, and electrical power from thermoelectric modules, fans, and pumps in each test are measured using a watt meter. The water flow rate was varied by 0.4 lpm, 0.5 lpm, and 0.6 lpm by adjusting the pump voltage within 5, 6, and 7 volts. The water temperature in and out of the water block was measured with a K-type thermocouple. Air velocity on the cold and hot sides of the ducting was measured with an anemometer.

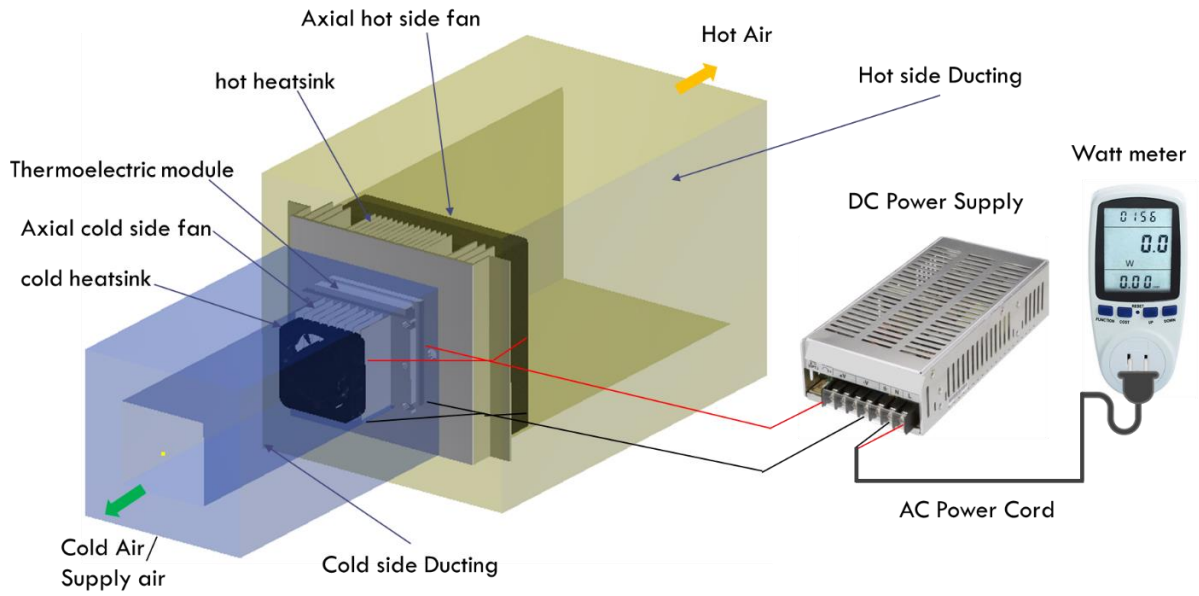

Figure 2. Prototype test model (without liquid block)

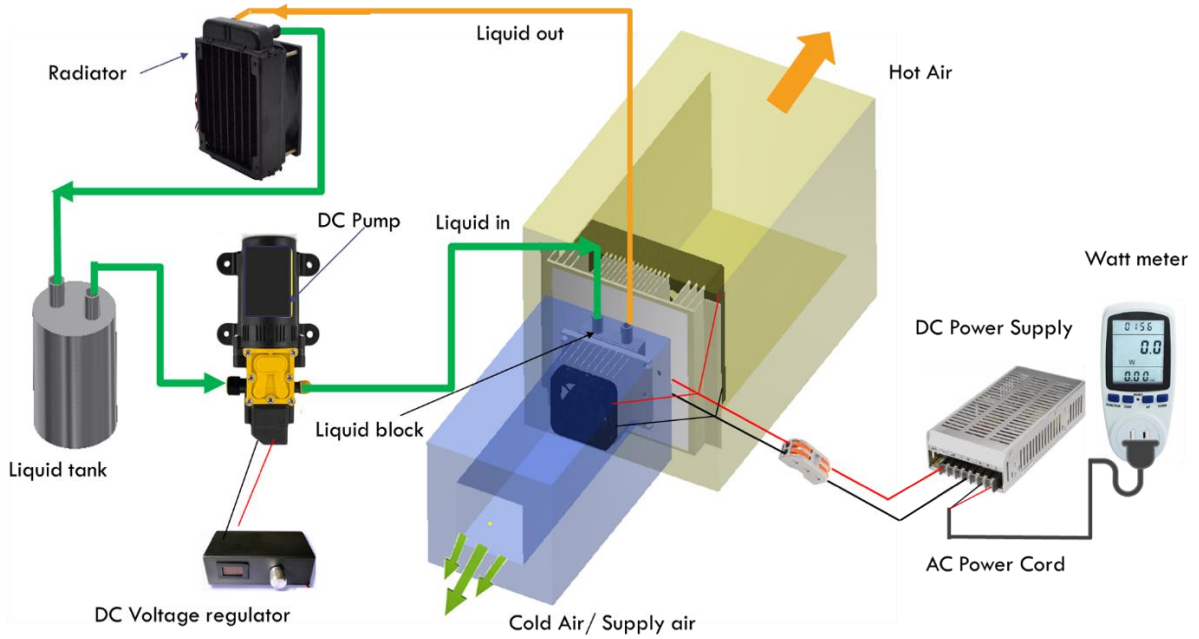

Figure 3. Prototype test model (with liquid block)

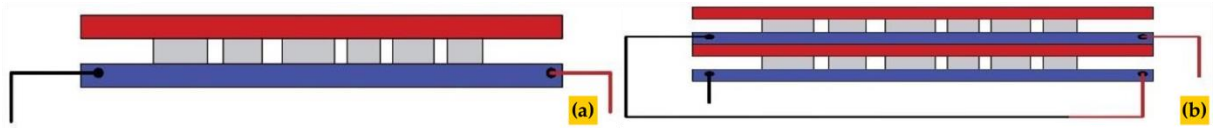

Figure 4. Thermoelectric arrangement: (a) Single thermoelectric; (b) Double thermoelectric, which is arranged in a series of electrical and parallel thermal arrangements

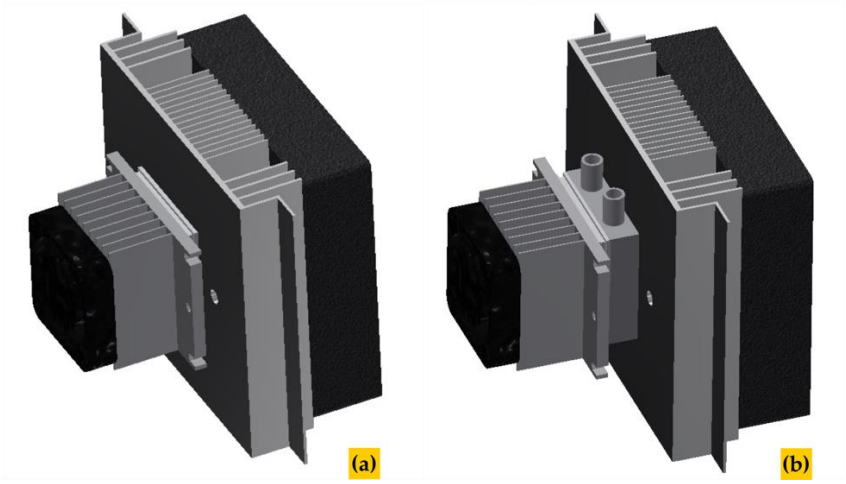

Figure 5. The thermoelectric cooling system's configuration: (a) Aluminum heatsink only; (b) A combination of aluminum heatsinks, and liquid block (b).

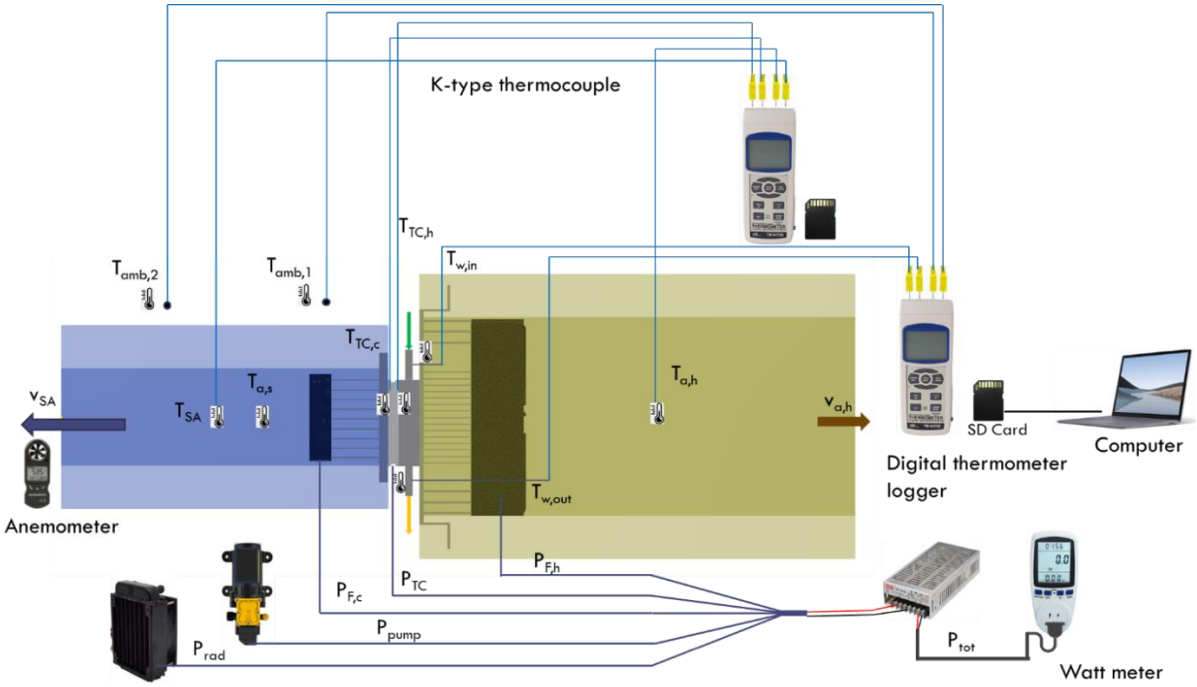

Figure 6. Experimental setup

2.2. *Thermoelectric Cooling Performance*

The performance of a thermoelectric cooler can be expressed by the Coefficient of performance (COP), as in Eq. (1) and Eq. (2) [34], [35].

$$COP_{TEC} = \frac{Cooling\ capacity}{Electrical\ input\ power} \quad (1)$$

$$COP_{TEC} = \frac{\dot{q}_c}{P_{tot}} \quad (2)$$

The cooling capacity of a thermoelectric cooler ($\dot{Q}_c$) can be determined by the total heat of the airflow through the cold-side heatsink [34], as shown in Eq. (3).

$$\dot{q}_c = \dot{m}_a C_{pa}(T_{a,s} - T_{SA}) \quad (3)$$

where $\dot{m}_a$ is the mass flow rate of air in the cold side ducting, C_{pa} is the air-specific heat, $T_{a,s}$ and T_{SA} are the air temperature in start condition and supply air temperatures of the cold side ducting, respectively.

The total input electrical power (P) to the thermoelectric cooling system [34] can be determined by Eq. (4).

$$P = P_{TEC+}\, P_{h+}\, P_c + P_{pump+}\, P_{rad} \quad (4)$$

P_{TEC} is the thermoelectric module's electrical power, P_h and P_c are the fan's electrical power on

the hot side and cold side of the thermoelectric, respectively, P_{pump} is pump electrical power and P_{rad} is radiator fan pump electrical power.

3. Results and Discussion

3.1. Profil Temperature

Figure 7a shows the profile temperature of the thermoelectric cooling system of a single TEC with a heatsink. $T_{TEC,h}$ and $T_{TEC,c}$ represent the hot and cold side TEC temperatures, respectively. $T_{a,h}$ is the air temperature in the hot side ducting, T_{SA} is the supply air temperature that will flow into the car cabin, and T_{amb} is the ambient air temperature. Data was collected for 2 hours (7200 minutes) for each variation, assuming the car was parked for 2 hours. In Figure 7a, $T_{TEC,h}$, and $T_{a,h}$ show an increase with time from 0 to 1000 s. The increase of $T_{TEC,h}$ and $T_{a,h}$ is due to the release of heat from the cold side to the hot side of TEC, which then flows through the hot side ducting, $T_{a,h}$. The TEC cold side temperature $T_{TEC,c}$ continues to decrease from the ambient temperature until it reaches 14.5 °C, and T_{SA} reaches 21.4 at 130 s, and then rises again until 1000 seconds. Overall, the temperatures of $T_{TEC,h}$, $T_{TEC,c}$, $T_{a,h}$, T_{SA}, and T_{amb} tend to be steady from 1000 to 7200 s. The electric current flows into the TEC module when connected to the power source, and due to the Peltier effect, heat is transferred from one side to another side of the TEC surface [36]. In the initial condition, the Peltier module has not yet operated at its maximum efficiency, so the temperature continues to drop to the lowest point on the cold side of the TEC. On the hot side, it also continues to rise at the highest temperature until a steady state, which aligns with the research of Remeli et al. [36].

The temperature profile of $T_{TEC,h}$ and $T_{a,h,}$ which sometimes rises from 0-1000 s, and the temperature of $T_{TEC,c}$, T_{SA}, which drops to 1000 s and then constant, is in line with research conducted by Mirmanto et al. [17] and Gökçek and Şahin [37]. The profile temperatures show that thermoelectric cooling can work properly for 2 hours to produce cold air in the cabin. A thermoelectric that can work constantly for 2 hours shows that this thermoelectric cooling can be applied to parked cars. The total power required by the thermoelectric cooling system, which consists of a single TEC and heatsink, is 53.3 W. Thermoelectric cooling using a single TEC with a heatsink can reduce the temperature by 7.3 °C from an average ambient temperature T_{amb} of 31.6 °C to an average supply air temperature T_{SA} of 24.3 °C. The supply air temperature, which initially has the same value as the ambient temperature Tamb = 31.6 °C, is passed on the cold side of the TEC and heatsink, which has a temperature $T_{TEC,c}$ = 14.5 °C. Because there is a temperature difference between both states, heat transfer occurs so that the Supply T_{SA} temperature becomes cooler to 24.3 °C. The heat from the T_{SA} air will be transferred to the cold side of the TEC and discharged through the hot side of the TEC Module and heatsink to the environment. This process of transferring heat and cooling the supply air temperature (TSA) will continue to work as long as there is power input to the TEC module [38]–[41]. This supply air temperature (TSA) will be blown to the evaporator side in the cabin of the parked car.

The temperature profile of the thermoelectric cooling system testing double TEC in a series electric-parallel thermal arrangement with the heatsink is shown in Figure 7b. In this configuration, the total power for the cooling system is 33.5 W. The temperatures of $T_{TEC,h,}$ and $T_{a,h}$ show an increase with time at time 0 to 500 s. The temperatures of $T_{TEC,c}$ and T_{SA} continue to decrease from seconds 0 to 500 s, while the ambient temperature tends to be relatively constant around 32 °C. In this second test, the temperatures of $T_{TEC,h}$, $T_{TEC,c}$, $T_{a,h}$, T_{SA}, and T_{amb} tend to be stable from 500 to 7200 s. Like in the first test using a single TEC, thermoelectric cooling can work stably for 2 hours to produce cold supply air to the cabin, and a faster steady temperature is achieved.

The double TEC with heatsink cooling system can reduce the temperature by 7.1 °C from an average ambient temperature of 33.5 °C to an average T_{SA} of 24.7 °C. Compared to a single TEC module that can reduce the air temperature by 7.3 °C, the decrease in air temperature in 2 modules arranged in parallel thermal and electrical series is lower. This is because the power input of 2 modules arranged in parallel thermal and electrical series is lower than the single TEC. The arrangement of thermal parallel or stacked TEC modules causes the cooling load of the two modules to be divided into two because the 2nd Peltier will cool the first module that has cooled

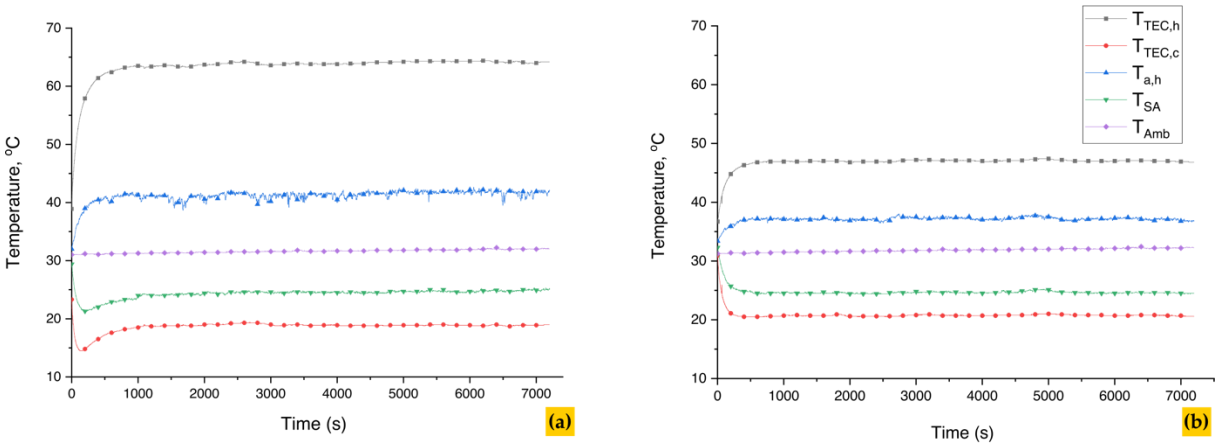

Figure 7. (a) Temperature profile of thermoelectric cooling: single TEC module with heatsink; (b) Double TEC module in series electric-parallel thermal arrangement with heatsink

first, lowering the power input. With a lower power input, causing the cooling capability to be slightly lower, the temperature on the cold side is an average of about 20.8 °C compared to 18.6 °C on the single TEC. The cooling capacity, which is only slightly different, but the power used is only 63% of the total power input when using a single TEC, shows that using an arrangement of 2 series and parallel thermal TEC modules is more efficient than a single TEC module.

3.2. *Effect of the Number of TEC Modules*

As the number of modules increases, the power input generated also increases [20], and indirectly impacts improving the performance of TEC modules in transferring heat and cooling capacity. However, this occurs in conditions where TEC modules are arranged in parallel electrically, where the total power input is a multiplication of the power input of each TEC module multiplied by the number of modules. It is different when the TEC modules are arranged in parallel thermal and electrical series, such as in **Figure 4**. The total power required by the thermoelectric cooling system consisting of a single TEC is 53.3 W. In comparison, the thermoelectric cooling system with dual TECs in a series thermal electric-parallel arrangement is 33.5 W.

In using a single TEC module, the entire cooling load is borne by one module, which causes the module to work harder to achieve the desired temperature, requiring higher electrical input power. In the double TEC arrangement in a series of electric-parallel thermals, the cooling load is divided equally between two modules, so each module only needs to handle part of the total load. It can be seen from the lower temperature gradient in each module, which reduces the workload and the need for electrical power. **Figure 7a** and **Figure 7b** show that using two TEC modules arranged in a series of electric-parallel thermal produces higher efficiency than a single TEC module. The cooling capacity produced is almost the same, but the power required by two TEC modules arranged in a series of electric-parallel thermal is only 63% of the single TEC module.

The arrangement of 2 TEC arranged electrically series and thermally parallel requires a smaller electric current for the same working voltage. The arrangement of thermoelectric in parallel is intended to maximize the heat transfer process so that cooling is maximized because the hot side of the first TEC will be cooled by the cold side of the second TEC so that the cold side of the first thermoelectric in direct contact with the air will be cooler. The TEC hot side temperature on the double TEC is lower, which is an average of 48.8 °C compared to the single TEC of 63.4 °C, which is proportional to the input power, where the double TEC is 33.5 W and the single TEC is 53.3 W. With the increase in input power, the TEC hot side temperature increases, which indicates that the higher the TEC temperature, the more heat is released to the heatsink side, and this condition is in line with Lertsatitthanakorn et al. [34].

3.3. *Impact of the Different Cooling Method*

In this study, a cooling water block is added on the hot side of the thermoelectric to improve the thermoelectric cooling performance. **Figure 8a**

shows the profile temperature of a single TEC, and **Figure 8b** shows the profile temperature of a double TEC, both are equipped with cooling water blocks with a fluid flow of 0.4 lpm. From **Figure 8a** and **Figure 8b**, adding a cooling water block increases the ability to dissipate heat faster on the TEC hot side. When the single TEC is without a cooling water block, the temperature on the TEC hot side averages 63.4 °C. The TEC hot side temperature averages 46.3 °C when adding the cooling water block. The decrease in temperature on the hot side of the thermoelectric $T_{TEC,h}$ is because some of the heat has been absorbed by water cooling. The decreasing TEC hot side temperature affects the cooling system's performance, making the thermoelectric cold side temperature cooler. In testing with a single TEC without a cooling water block, the average temperature is 18.6 °C. When a cooling water block is added, the temperature on the cold side reaches 12.0 °C, resulting in a supply temperature, T_{SA} to the cabin of 21.4 °C. Adding a cooling water block to the double TEC also has a significant effect. In the double TEC without cooling water block testing, the temperature on the TEC hot side reaches an average of 46.8 °C, and when adding a cooling water block, the average TEC hot side temperature is 45.3 °C. The cooling system using a double TEC with a heatsink can reduce the temperature on the cold side of the thermoelectric to reach 17.9 °C and produce a supply temperature to the cabin of 23.1 °C. The use of a single TEC provides a maximum cooling effect compared to the use of a double TEC, this is because the double TEC arranged in series electrical and parallel thermal provides lower current and electrical power with a difference of 19.8 W lower than single TEC. Adding a cooling water block increases the ability to dissipate heat faster on the hot side of the thermoelectric module, which impacts improving cooling performance.

In this study, the liquid flow rate of the water-ethylene glycol mixture was varied to 0.4 lpm, 0.5 lpm, and 0.6 lpm. The average temperature in each cooling system configuration is shown in **Figure 9**. The fluid flow rate of 0.5 lpm provides the highest cooling performance compared to 0.4 lpm and 0.6 lpm. A single TEC with a heatsink and 0.4 lpm cooling water produces the TEC cold side temperature reaches 12.0 °C, then at a water flow rate of 0.5 lpm the TEC cold side temperature reaches 11.1 °C, and at 0.6 lpm the TEC cold side temperature reaches 13.7 °C. The temperature on the TEC cold side produces supply temperature T_{SA} of 21.4 °C, 20.7 °C, and 22.1 °C, respectively. A flow rate of 0.4 lpm has lower cooling performance because the flow rate of water to cool the TEC surface is too slow, so the water is less effective in absorbing heat from the hot side of the TEC. At the same time, the most optimal cooling performance occurs at a flow rate of 0.5 lpm, which is indicated by the TEC cold side temperature and the lowest supply air temperature. However, when the water flow rate is increased, the TEC cold side temperature and supply air temperature increase, causing the water flow rate to be too fast so that the water contact with the heat source is too short and results in less heat being absorbed, which is in line

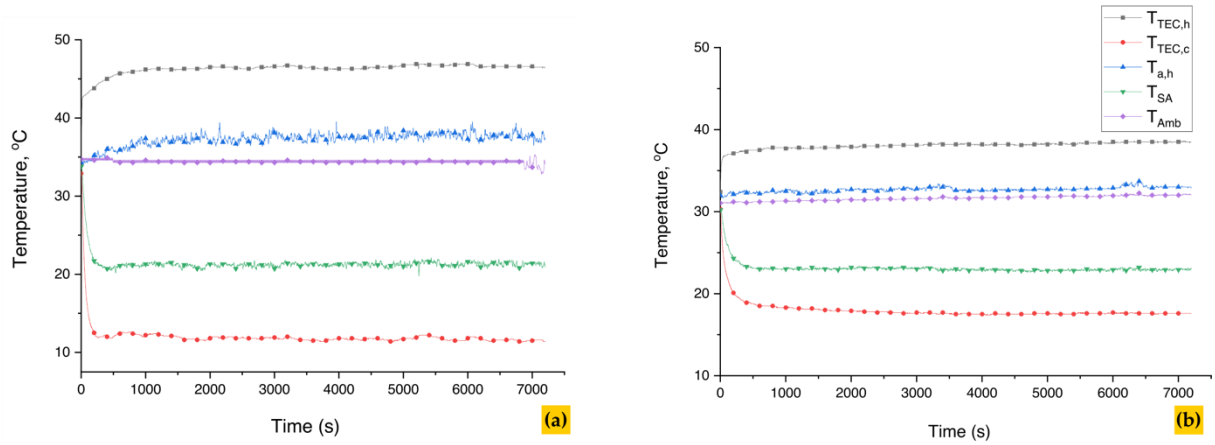

Figure 8. Thermoelectric cooling temperature profile at 5 lpm fluid flow rate: (a) Single TEC module with heatsink and cooling water block; (b) TEC module with heatsink and cooling water block

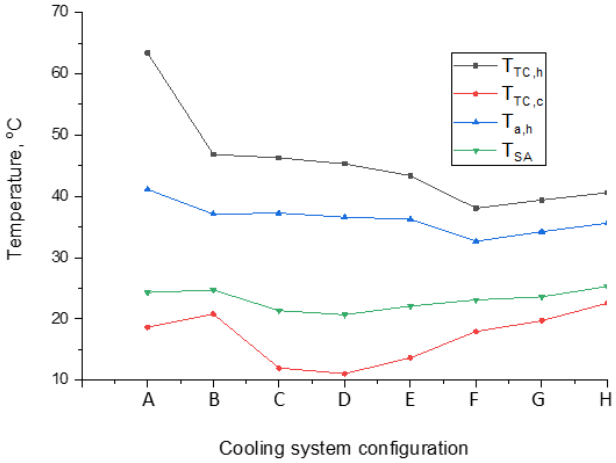

Figure 9. Average temperature in each cooling system configuration: (A) Single TEC+heatsink; (B) Double TEC+heatsink; (C) Single TEC+heatsink+0.4 lpm; (D) Single TEC+heatsink+0.5 lpm; (E) Single TEC+heatsink+0.6 lpm; (F) Double TEC+heatsink+0.4 lpm; (G) Double TEC+heatsink+0.5 lpm; (H) Double TEC+heatsink+0.6 lpm

with the research conducted by Atmoko et al. [12]. Performance improvement from using water cooling also occurs in the double TEC cooling system, where water cooling with a flow rate of 0.5 lpm produces the lowest thermoelectric cold side temperature and supply air temperature of 19.7 °C and 23.6 °C.

3.4. Cooling Performance

Table 1 shows the effect of cooling system configuration on hot-side and cold-side TEC temperatures, TEC input power, total cooling system input power, cooling capacity, and COP. The cooling capacity is determined by Eq. (3) by involving the difference in temperature of the cold-side ducting at the initial condition before cooling and the supply temperature on average. The measurement results show that the air temperature in the cold channel in the initial condition before cooling is equivalent to the average ambient temperature, so the cooling capacity calculation uses the temperature difference at ambient temperature and supply temperature (T_{amb} - T_{SA}).

Using a single TEC requires a greater input power than a double TEC arranged in electrical series and thermal parallel, where the single TEC is 42.4 W while the double TEC is 22.6 W. This affects the performance of the TEC, where the higher the input power, the higher the hot side of TEC temperature. The higher temperature on the hot side TEC shows greater heat dissipation, resulting in a lower temperature on the cold side. With a relatively constant ambient temperature of around ~32 °C, the lower cold side TEC temperature will produce a lower supply temperature (T_{SA}) and greater cooling capacity. Cooling capacity is a function of the difference between ambient temperature (T_{amb}) and supply temperature (T_{SA}) obtained to flow into the car cabin, which is obtained using Eq. (3). As shown in **Table 1** and **Figure 10**, the cooling capacity of the single TEC is 28.2 W and the double TEC produces 27.5 °C. The addition of a cooling water block provides an increase in cooling capacity. Using a cooling water block as an additional cooling system increases heat transfer performance, as shown by the heat absorption from the hot side of the TEC module, and the discharge into the environment is higher. This causes the temperature on the cold side of the TEC module to be lower. With the lower temperature of the cold side TEC module, the supply temperature (T_{SA}) that passes through the cold side becomes lower, causing a higher decrease in the supply air temperature (T_{SA}). The higher the difference in air supply temperature to the car cabin, the greater the cooling capacity generated. At the same power input, the higher the cooling capacity, the higher the coefficient of performance of the cooling system. The highest cooling capacity is 51.3 W when using a single TEC with an aluminum heatsink and 0.5 lpm cooling water.

Figure 11 shows the COP for several cooling system configurations. COP is calculated based on Eq. (1) and Eq. (2), which is the ratio of cooling capacity divided by total input power. The cooling capacity on a single TEC is indeed higher than on a double TEC. Still, because the total input power is almost 2 times greater than double

thermoelectric, the COP on a single TEC is lower. The highest COP of 0.84 was obtained in the double TEC with heatsink and added 0.5 lpm water cooling system, while the lowest COP of 0.53 occurred in the single thermoelectric configuration with heatsink only [42].

Table 1. Hot-side and cold-side TEC temperatures, thermoelectric cooler input power, total cooling system input power, the cooling capacity, and COP for various Cooling system configurations ($\dot{m}_a$ =3.84 g/s).

Cooling System Configuration	$T_{TEC,h}$ (°C)	$T_{TEC,c}$ (°C)	TEC Input Power (W)	Total Input power (W)	Cooling Capacity Qc (W)	COP
Single TEC+heatsink	63.4	18.6	42.4	53.3	28.2	0.53
Double TEC+heatsink	46.8	20.8	22.6	33.5	27.5	0.82
Single TEC+heatsink+0.4 lpm	46.3	12.0	42.4	60.9	50.2	0.82
Single TEC+heatsink+0.5 lpm	45.3	11.1	42.4	62.6	51.3	0.82
Single TEC+heatsink+0.6 lpm	43.4	13.7	42.4	64.0	43.9	0.69
Double TEC+heatsink+0.4 lpm	38.1	17.9	22.6	41.2	33.0	0.80
Double TEC+heatsink+0.5 lpm	39.4	19.7	22.6	41.9	35.0	0.84
Double TEC+heatsink+0.6 lpm	40.6	22.6	22.6	43.1	32.0	0.74

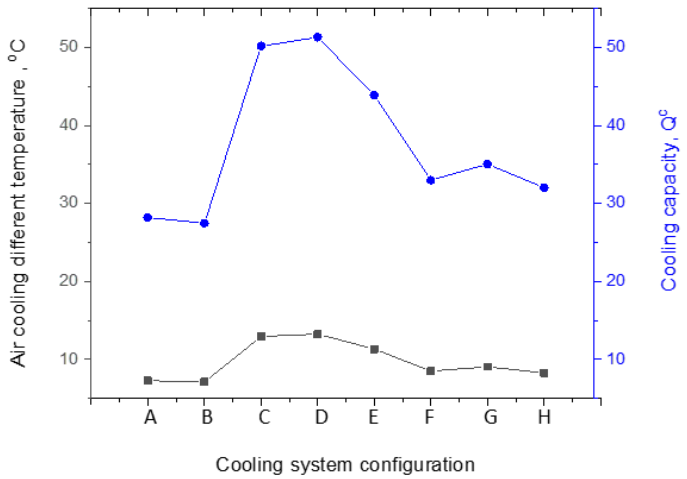

Figure 10. Cooling capacity: (A) Single TEC+heatsink; (B) Double TEC+heatsink; (C) Single TEC+heatsink+0.4 lpm; (D) Single TEC+heatsink+0.5 lpm; (E) Single TEC+heatsink+0.6 lpm; (F) Double TEC+heatsink+0.4 lpm; (G) Double TEC+heatsink+0.5 lpm; (H) Double TEC+heatsink+0.6 lpm

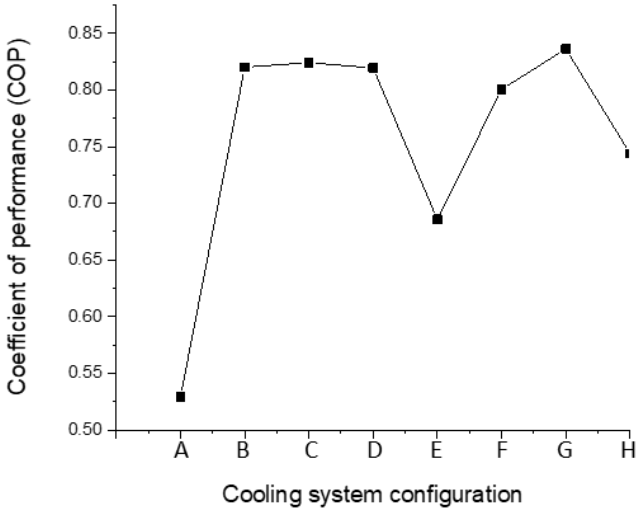

Figure 11. Coefficient of performance (COP): (A) Single TEC+heatsink; (B) Double TEC+heatsink; (C) Single TEC+heatsink+0.4 lpm; (D) Single TEC+heatsink+0.5 lpm; (E) Single TEC+heatsink+0.6 lpm; (F) Double TEC+heatsink+0.4 lpm; (G) Double TEC+heatsink+0.5 lpm; (H) Double TEC+heatsink+0.6 lpm

3.5. *Uncertainty Analysis*

The temperature of T_{amb} and T_{SA} are measured with the K-type thermocouple connected to the LUTRON TM-947SD digital thermometer. The temperature calibration was conducted, and the error associated with (T_{amb} - T_{SA}) was ±0.3 °C. The cooling capacity of thermoelectric cooling can be determined in Eq. (3). The uncertainties of the cooling capacity ($S_{\dot{Q}_c} / \dot{Q}_c$) and Coefficient of performance (S_{COP}/COP) can be estimated as Eq. (5) and Eq. (6), respectively, with the assumption that there is no change in the ducting area (A), air density (ϱ), and specific heat (Cp) are constant [43]–[46]. The air velocity in the cold side of the ducting was measured using an anemometer sensor with an accuracy of ± 0.1 m/s. The total power used to operate the thermoelectric cooling system was measured with a digital watt meter with an accuracy of ±0.1W.

$$\frac{S_{\dot{Q}_c}}{\dot{Q}_c} = \sqrt{\left(\frac{S_v}{v}\right)^2 + \left(\frac{S(T_{amb} - T_{SA})}{(T_{amb} - T_{SA})}\right)^2} \quad (5)$$

$$\frac{S_{COP}}{COP} = \sqrt{\left(\frac{S_v}{v}\right)^2 + \left(\frac{S(T_{amb} - T_{SA})}{(T_{amb} - T_{SA})}\right)^2 + \left(\frac{S_P}{P}\right)^2} \quad (6)$$

The maximum uncertainty of cooling capacity ($S_{\dot{Q}_c} / \dot{Q}_c$) and Coefficient of performance (S_{COP}/COP) determined based on Eq. (5) and Eq. (6) and were found to be ±5.3% and ± 6.5% respectively.

4. Conclusion

The thermoelectric cooling system, which produces cold supply air to the car cabin, can work properly during the 2-hour test, and it constantly produces a supply temperature to the cabin space between 20-25 °C, depending on the configuration of the cooling system. Using a single TEC module delivers a greater power input than a double TEC module arranged in electrical series and thermal parallel, and the higher the input power produced, the higher the cooling capacity. Adding a cooling water block provides improved cooling system performance, indicated by an increase in cooling capacity compared to not using a cooling water block. The highest cooling capacity of 51.3 W was obtained when using a single TEC with an aluminum heatsink and 0.5 lpm cooling water block, and the lowest of 27.5 W was obtained when using double TEC modules without a cooling water block. The overall performance of the cooling system is a function of cooling capacity and input power. Although the use of a single thermoelectric produces a higher cooling capacity, the input power used is almost twice, so the COP of the cooling system using a double TEC is higher. The highest COP of 0.84 was obtained in the double TEC configuration with heatsink and added 0.5 lpm water cooling system, while the lowest COP of 0.53 occurred in the single thermoelectric configuration with heatsink only. Therefore, a double TEC module configuration arranged in an electrical series and thermal parallel and an added 0.5 lpm cooling water block could be recommended for cooling the cabin of a parked car. Depending on the required car cooling capacity, the number of cooling system arrays can be determined by dividing the total cooling load by one cooling system's cooling capacity, consisting of a double TEC module configuration and a cooling water block.

Acknowledgements

The authors would like to thank the Institute of Research and Community Service Universitas Negeri Jakarta for funding this research through the National Collaborative Research in 2023 with grant number No: 49/KN/LPPM/III/2023.

Author's Declaration

Authors' contributions and responsibilities

The authors made substantial contributions to the conception and design of the study. The authors took responsibility for data analysis, interpretation and discussion of results. The authors read and approved the final manuscript.

Funding

This research was funded by the Institute for Research and Community Service of Universitas Negeri Jakarta with grant number No: 49/KN/LPPM/III/2023.

Availability of data and materials

All data are available from the authors.

Competing interests

The authors declare no competing interest.

Additional information

No additional information from the authors.

References

[1] R. S. Srivastava, A. Kumar, H. Thakur, and R. Vaish, "Solar assisted thermoelectric

cooling/heating system for vehicle cabin during parking: A numerical study," *Renewable Energy*, vol. 181, pp. 384–403, Jan. 2022, doi: 10.1016/j.renene.2021.09.063.

[2] R. Sukarno, A. Premono, Y. Gunawan, and A. Wiyono, "Experimental study of thermoelectric cooling system for a parked car with solar energy," *Journal of Physics: Conference Series*, vol. 2596, no. 1, p. 012052, Sep. 2023, doi: 10.1088/1742-6596/2596/1/012052.

[3] R. Sukarno, N. Putra, and I. I. Hakim, "Non-dimensional analysis for heat pipe characteristics in the heat pipe heat exchanger as energy recovery device in the HVAC systems," *Thermal Science and Engineering Progress*, vol. 26, p. 101122, Dec. 2021, doi: 10.1016/j.tsep.2021.101122.

[4] R. Sukarno, N. Putra, I. I. Hakim, F. F. Rachman, and T. M. I. Mahlia, "Multi-stage heat-pipe heat exchanger for improving energy efficiency of the HVAC system in a hospital operating room 1," *International Journal of Low-Carbon Technologies*, vol. 16, no. 2, pp. 259–267, May 2021, doi: 10.1093/ijlct/ctaa048.

[5] I. I. Hakim, N. Putra, R. Sukarno, M. R. Audi, and F. F. Rachman, "Experimental study on utilization of heat pipe heat exchanger for energy conservation of air conditioning system in a hospitals and its techno-economic feasibility," in *The 4th International Tropical Renewable Energy Conference (I-TREC 2019)*, 2020, p. 030067. doi: 10.1063/5.0014138.

[6] M. Setiyo, B. Waluyo, N. Widodo, M. L. Rochman, S. Munahar, and S. D. Fatmaryanti, "Cooling effect and heat index (HI) assessment on car cabin cooler powered by solar panel in parked car," *Case Studies in Thermal Engineering*, vol. 28, p. 101386, Dec. 2021, doi: 10.1016/j.csite.2021.101386.

[7] C.-Q. Su, Z.-Z. Wang, X. Liu, X. Xiong, T. Jiang, and Y.-P. Wang, "Research on thermal comfort of commercial vehicle and economy of localized air conditioning system with thermoelectric coolers," *Energy Reports*, vol. 8, pp. 795–803, Nov. 2022, doi: 10.1016/j.egyr.2022.10.153.

[8] Q. Wan, C. Su, X. Yuan, L. Tian, Z. Shen, and X. Liu, "Assessment of a Truck Localized Air Conditioning System with Thermoelectric Coolers," *Journal of Electronic Materials*, vol. 48, no. 9, pp. 5453–5463, Sep. 2019, doi: 10.1007/s11664-019-06983-4.

[9] R. Guráš, M. Mahdal, and M. Bojko, "Heat transfer analysis of a liquid cooling device using thermoelectric elements," *Applied Thermal Engineering*, vol. 226, p. 120274, May 2023, doi: 10.1016/j.applthermaleng.2023.120274.

[10] C. Chen, L. Mao, T. Lin, T. Tu, L. Zhu, and C. Wang, "Performance testing and optimization of a thermoelectric elevator car air conditioner," *Case Studies in Thermal Engineering*, vol. 19, p. 100616, Jun. 2020, doi: 10.1016/j.csite.2020.100616.

[11] D. Champier, "Thermoelectric generators: A review of applications," *Energy Conversion and Management*, vol. 140, pp. 167–181, May 2017, doi: 10.1016/j.enconman.2017.02.070.

[12] N. T. Atmoko, A. Jamaldi, and T. W. B. Riyadi, "An Experimental Study of the TEG Performance using Cooling Systems of Waterblock and Heatsink-Fan," *Automotive Experiences*, vol. 5, no. 3, pp. 261–267, Jun. 2022, doi: 10.31603/ae.6250.

[13] Y. Sun, F. Meng, B. San, and C. Xu, "Performance Analysis of Multistage Thermoelectric Cooler with Water-Cooled," *Journal of Physics: Conference Series*, vol. 2442, no. 1, p. 012028, Feb. 2023, doi: 10.1088/1742-6596/2442/1/012028.

[14] H. Yang, H. Zhao, and G. Xia, "Performance analysis of multi thermoelectric cooling modules," *Journal of Physics: Conference Series*, vol. 2030, no. 1, p. 012015, Sep. 2021, doi: 10.1088/1742-6596/2030/1/012015.

[15] S. Wiriyasart, P. Suksusron, C. Hommalee, A. Siricharoenpanich, and P. Naphon, "Heat transfer enhancement of thermoelectric cooling module with nanofluid and ferrofluid as base fluids," *Case Studies in Thermal Engineering*, vol. 24, p. 100877, Apr. 2021, doi: 10.1016/j.csite.2021.100877.

[16] Y. Cai, Y. Wang, D. Liu, and F.-Y. Zhao, "Thermoelectric cooling technology applied in the field of electronic devices: Updated review on the parametric investigations and model developments," *Applied Thermal Engineering*, vol. 148, pp. 238–255, Feb. 2019,

doi: 10.1016/j.applthermaleng.2018.11.014.

[17] M. Mirmanto, S. Syahrul, and Y. Wirdan, "Experimental performances of a thermoelectric cooler box with thermoelectric position variations," *Engineering Science and Technology, an International Journal*, vol. 22, no. 1, pp. 177–184, Feb. 2019, doi: 10.1016/j.jestch.2018.09.006.

[18] K. Ma, Z. Zuo, and W. Wang, "Design and experimental study of an outdoor portable thermoelectric air-conditioning system," *Applied Thermal Engineering*, vol. 219, p. 119471, Jan. 2023, doi: 10.1016/j.applthermaleng.2022.119471.

[19] E. Y. M. Ang, P. S. Ng, C. B. Soh, and P. C. Wang, "Multi-stage thermoelectric coolers for cooling wearables," *Thermal Science and Engineering Progress*, vol. 36, p. 101511, Dec. 2022, doi: 10.1016/j.tsep.2022.101511.

[20] H. A. Ahmed, T. F. Megahed, S. Mori, S. Nada, and H. Hassan, "Performance investigation of new design thermoelectric air conditioning system for electric vehicles," *International Journal of Thermal Sciences*, vol. 191, p. 108356, Sep. 2023, doi: 10.1016/j.ijthermalsci.2023.108356.

[21] C. Qiu and W. Shi, "Comprehensive modeling for optimized design of a thermoelectric cooler with non-constant cross-section: Theoretical considerations," *Applied Thermal Engineering*, vol. 176, p. 115384, Jul. 2020, doi: 10.1016/j.applthermaleng.2020.115384.

[22] J. Chen, R. Wang, D. Luo, and W. Zhou, "Performance optimization of a segmented converging thermoelectric generator for waste heat recovery," *Applied Thermal Engineering*, vol. 202, p. 117843, Feb. 2022, doi: 10.1016/j.applthermaleng.2021.117843.

[23] Z. Liu *et al.*, "Design and optimization of a cubic two-stage thermoelectric cooler for thermal performance enhancement," *Energy Conversion and Management*, vol. 271, p. 116259, Nov. 2022, doi: 10.1016/j.enconman.2022.116259.

[24] A. Winarta, I. M. Rasta, I. N. Suamir, and I. G. K. Puja, "Experimental Study of Thermoelectric Cooler Box Using Heat Sink with Vapor Chamber as Hot Side Cooling Device," in *Proceedings of the 2nd International Conference on Experimental and Computational Mechanics in Engineering*, 2021, pp. 389–399. doi: 10.1007/978-981-16-0736-3_37.

[25] L. P. I. Midiani, I. W. A. Subagia, I. W. Suastawa, A. A. N. G. Sapteka, and A. Winarta, "Preliminary investigation of performance and temperature distribution of thermoelectric cooler box with and without internal fan," *Journal of Physics: Conference Series*, vol. 1450, no. 1, p. 012088, Feb. 2020, doi: 10.1088/1742-6596/1450/1/012088.

[26] A. Elarusi, A. Attar, and H. Lee, "Optimal Design of a Thermoelectric Cooling/Heating System for Car Seat Climate Control (CSCC)," *Journal of Electronic Materials*, vol. 46, no. 4, pp. 1984–1995, Apr. 2017, doi: 10.1007/s11664-016-5043-y.

[27] C. Su, W. Dong, Y. Deng, Y. Wang, and X. Liu, "Numerical and Experimental Investigation on the Performance of a Thermoelectric Cooling Automotive Seat," *Journal of Electronic Materials*, vol. 47, no. 6, pp. 3218–3229, Jun. 2018, doi: 10.1007/s11664-017-5960-4.

[28] D. Kim *et al.*, "Design and performance analyses of thermoelectric coolers and power generators for automobiles," *Sustainable Energy Technologies and Assessments*, vol. 51, p. 101955, Jun. 2022, doi: 10.1016/j.seta.2022.101955.

[29] Q. R. Al-Amir, M. F. Al-Dawody, and A. muhson Abd, "Design of Cooling System for an Automotive using Exhaust Gasses of Turbocharged Diesel Engine," *Journal of The Institution of Engineers (India): Series C*, vol. 103, no. 3, pp. 325–337, Jun. 2022, doi: 10.1007/s40032-021-00787-4.

[30] C. Harsito, Mufti Reza Aulia Putra, Daniel Aquino Purba, and T. Triyono, "Mini Review of Thermoelectric and their Potential Applications as Coolant in Electric Vehicles to Improve System Efficiency," *Evergreen*, vol. 10, no. 1, pp. 469–479, Mar. 2023, doi: 10.5109/6782150.

[31] Testing Autos, "Car heating system: how it works," *Testing Autos*, 2020. https://www.testingautos.com/car_care/car-heating-system.html

[32] X. Li, C. Zou, and A. Qi, "Experimental study on the thermo-physical properties of car

engine coolant (water/ethylene glycol mixture type) based SiC nanofluids," *International Communications in Heat and Mass Transfer*, vol. 77, pp. 159–164, Oct. 2016, doi: 10.1016/j.icheatmasstransfer.2016.08.009.

[33] N. Santhi Sree, A. Kalyan Charan, M. Harshitha Vaishnavi, M. Haritha Chinmayi, and J. Nikhil, "Analysis of radiator with different working fluids as coolants," in *Materials Today: Proceedings*, Mar. 2023. doi: 10.1016/j.matpr.2023.03.395.

[34] C. Lertsatitthanakorn, P. Bamroongkhan, and J. Jamradloedluk, "Performance study of thermoelectric dehumidification system integrated with heat pipe heatsink," *Results in Engineering*, vol. 17, p. 100901, Mar. 2023, doi: 10.1016/j.rineng.2023.100901.

[35] N. P. Bayendang, M. T. Kahn, and V. Balyan, "A Structural Review of Thermoelectricity for Fuel Cell CCHP Applications," *Journal of Energy*, vol. 2020, pp. 1–23, Jul. 2020, doi: 10.1155/2020/2760140.

[36] M. Fairuz Remeli, N. Ezzah Bakaruddin, S. Shawal, H. Husin, M. Fauzi Othman, and B. Singh, "Experimental study of a mini cooler by using Peltier thermoelectric cell," *IOP Conference Series: Materials Science and Engineering*, vol. 788, no. 1, p. 012076, Apr. 2020, doi: 10.1088/1757-899X/788/1/012076.

[37] M. Gökçek and F. Şahin, "Experimental performance investigation of minichannel water cooled-thermoelectric refrigerator," *Case Studies in Thermal Engineering*, vol. 10, pp. 54–62, Sep. 2017, doi: 10.1016/j.csite.2017.03.004.

[38] J. Yang, W. Liang, J. Han, R. Wu, and Y. Su, "Experimental study on a novel split thermoelectric cooler of big temperature difference for combined cooling and heating supply," *Energy Conversion and Management*, vol. 317, p. 118847, Oct. 2024, doi: 10.1016/j.enconman.2024.118847.

[39] J. Yang, C. Mou, J. Han, Y. Ge, W. Zhu, and W. Liang, "Investigation on performance of a new thermoelectric cooler with hot and cold side separation for suppressing Fourier effect," *Energy Conversion and Management*, vol. 298, p. 117760, Dec. 2023, doi: 10.1016/j.enconman.2023.117760.

[40] J. Wang, P. Cao, X. Li, X. Song, C. Zhao, and L. Zhu, "Experimental study on the influence of Peltier effect on the output performance of thermoelectric generator and deviation of maximum power point," *Energy Conversion and Management*, vol. 200, p. 112074, Nov. 2019, doi: 10.1016/j.enconman.2019.112074.

[41] Z. He, Q. Yu, J. Ye, F. Yan, and Y. Li, "Optimization of plate-fin heat exchanger performance for heat dissipation of thermoelectric cooler," *Case Studies in Thermal Engineering*, vol. 53, p. 103953, Jan. 2024, doi: 10.1016/j.csite.2023.103953.

[42] Y. Thimont and S. LeBlanc, "The impact of thermoelectric leg geometries on thermal resistance and power output," *Journal of Applied Physics*, vol. 126, no. 9, Sep. 2019, doi: 10.1063/1.5115044.

[43] X. Cui, Y. Zhu, Z. Li, and S. Shun, "Combination study of operation characteristics and heat transfer mechanism for pulsating heat pipe," *Applied Thermal Engineering*, vol. 65, no. 1–2, pp. 394–402, Apr. 2014, doi: 10.1016/j.applthermaleng.2014.01.030.

[44] V. K. Karthikeyan, K. Ramachandran, B. C. Pillai, and A. Brusly Solomon, "Effect of nanofluids on thermal performance of closed loop pulsating heat pipe," *Experimental Thermal and Fluid Science*, vol. 54, pp. 171–178, Apr. 2014, doi: 10.1016/j.expthermflusci.2014.02.007.

[45] R. Sukarno, N. Putra, I. I. Hakim, F. F. Rachman, and T. M. Indra Mahlia, "Utilizing heat pipe heat exchanger to reduce the energy consumption of airborne infection isolation hospital room HVAC system," *Journal of Building Engineering*, vol. 35, p. 102116, Mar. 2021, doi: 10.1016/j.jobe.2020.102116.

[46] H. Jouhara and R. Meskimmon, "An investigation into the use of water as a working fluid in wraparound loop heat pipe heat exchanger for applications in energy efficient HVAC systems," *Energy*, vol. 156, pp. 597–605, Aug. 2018, doi: 10.1016/j.energy.2018.05.134.